KINETIC AND THERMODYNAMIC STUDIES OF THE ADSORPTION OF LEAD (II) AND ZINC (II) IONS ONTO COCKLE SHELL POWDER

Supported by tetfund TERTIARY EDUCATION TRUST FUND

D.T. Ayodele and F.A. Adekola*
Department of Industrial Chemistry, University of Ilorin, PMB 1515, Ilorin, Nigeria
*Correspondence author: fadekola@hotmail.com

Abstract: This study examined the suitability of cockle shell (CS) powder in the removal of Pb^{2+} and Zn^{2+} metal ions. The high rate of discharge of heavy metals often regarded as cumulative poisons into the environment through industrial processes and metallic waste prompted this research. The properties of this calcareous adsorbent were characterized by X-ray diffraction (XRD), X-ray fluorescence (XRF), scanning electron microscopy (SEM), Brunauer–Emmett–Teller (BET) channel structure measurements and Fourier Transform Infrared spectrometry (FTIR). The influences of concentration, pH, contact time, adsorbent dose and temperature on the sorption capacity of these adsorbents were investigated. The results revealed cockle shell as a good adsorben t for both Pb^{2+} and Zn^{2+} ions in aqueous media with both ions exhibiting competitive adsorption behaviour. At a solution concentration of 100 mg/L, Pb^{2+} and Zn^{2+} uptake by cockle shell were 24.66 and 21.70 mg/g, respectively. The adsorption of these metal ions was modelled using Langmuir, Freundlich, Temkin and Dubinin-Raduskevich isotherms. Freundlich and Dubinin-Radushkevichisotherms adequately described the sorption Zn^{2+} and Pb^{2+}, respectively by the cockle shell. The thermodynamics and kinetics studies also revealed that the adsorption process was endothermic in nature and followed pseudo second order.

Keywords: Biosorbent; calcareous and cockle shell; heavy metal ions; sorption equilibrium.

Introduction

Contamination of the environment by heavy metals has been on the increase due to industrial revolution of the last few decades. Inevitably, industrial processes and spent commercial metallic products generate large quantity of metallic wastes, which are discharged into the water or land-dump sites (Abdus-Salam and Adekola, 2005). Consequently, there has been adverse effect on our environment, because of the toxicity of these heavy metals. They are considered cumulative poisons due to the fact that they accumulate in living things any time they are taken up and are stored faster than they are broken down (metabolized) or excreted (Wikipedia, 2013). This gives rise to the growing concern on the gradual build-up of toxic metals in the ecosystem. Although, heavy metal removal methods based on the principle of ion exchange, chemical precipitation, coagulation, etc, have evolved in the past, the risk of generating secondary pollutants by these methods is of great concern. Consequently, the use of biological materials for metal removal which reduces the possibilities of yielding unwanted chemicals has been promoted (Abdus-Salam and Adekola, 2005). Application of calcareous shells in metal adsorption (Gifford *et al.*, 2006) has been investigated as evident from the studies on snail shell (Asif and Gautam, 2013), bivalve shell (Liu *et al.*, 2009; Pena-Rodriguez *et al.*, 2010) and the crab and acra shell biomass (Dahiya *et al.*, 2008). These studies have demonstrated that unlike other approaches, calcium carbonate derivatives may be a potential cost-effective sorbent for removal of heavy metals. Shells of the fresh and sea waters can be considered as a cheap source of calcium carbonate, and thus the shells can be considered as biosorbent. This hypothesis was put to test by the present study which is aimed at evaluating the suitability of cockle shell powder as an adsorbent for lead and zinc ions.

Materials and Methods

Preparation of the adsorbent

The cockle shells used were obtained from a major market in Ilorin, Kwara State, Nigeria. These shells were thoroughly washed to remove the dirt and were rinsed with deionised water. The cockle shells were then charred in a furnace at 650℃ for 1 h. The charred shells were then ground into powdered form using a mortar and pestle and exposed to free air for 3 h for cooling. This ground sample was then sieved using a sieve size of 90 µm. The obtained sample was kept in a container and stored at room temperature for further studies.

Preparation of metal solutions

The stock solutions were prepared from $Pb(NO_3)_2$ (Kem Light) and $ZnSO_4.7H_2O$ (BDH) salts. These salts were oven-dried at 105°C for 4 h after which 1.598 g of the lead salt and 4.395 g of the zinc salt were weighed and each dissolved in a 100 mL deionised water to which 1 mL of concentrated nitric acid was added. These were then diluted with deionized water up to 1000 mL. 1 mL contained 1 mg of the metal ion (1000 mg/L). Aliquots of these adsorbates containing varying concentrations from 10 ppm to 100 ppm were then prepared by dilution from their stock solutions for the adsorption studies.

Adsorption studies

The experiments were carried out in batch mode because of its relative simplicity. These batch experiments were run in flasks of the same capacity using a water bath constant temperature oscillator (SHA-B). Prior to each experiment, a pre-determined amount of adsorbent was added to each flask. The stirring was kept constant for each run throughout the experiment, ensuring equal mixing. The desired pH was maintained using 0.01M NaOH or 0.01M HCl solutions as the case may be. Each flask was then filled with 50 mL of sample having the desired pH before the agitation commenced. The flasks containing the samples were then withdrawn from the shaker at a predetermined time interval and filtered and the concentration of the residual metal ion was determined by Atomic Absorption Spectrophotometer. The influence of initial metal ion concentration was studied in the range of 10 – 100 mg/L. The effect of pH was performed by

varying the pH of the solution from 3 – 6. For the effect of contact time, a time range of 5 – 360 min was considered while 0.1 – 0.5 g dosage was considered for the effect of the adsorbent dosage. The effect of temperature was studied over a temperature range of 30 – 60℃. The amount of metal ion adsorbed during the series of batch investigations was determined using a mass balance equation (Badmus *et al.,* 2007*)* (Equation 1);

$$q_e = \frac{v}{m}(C_o - C_e) \ldots\ldots\ldots\ldots\ldots\ldots (1)$$

Where: q_e is the metal uptake (mg/g); C_o and C*e* are the initial and equilibrium metal concentrations in the sample (mg/L), respectively; v is the sample volume (L); and m is the mass of adsorbent used (g). The removal efficiency is as given in Equation 2;

$$RemovalEfficiency(\%) = \left(\frac{C_o - C_e}{C_o}\right) \times 100 \ldots\ldots (2)$$

Where: C_o and C*e* are the metal concentrations in the sample before and after treatment, respectively.

Characterization

The X-ray diffraction (XRD) pattern oftheCS powder was obtained using a PANalyticalX′Pert PRO MRD PW3040 diffractometer. Its chemical constituents weredetermined using a MINI PAL 4 Energy Dispersive X-ray fluorescence (XRF) spectrometer. The Brunauer-Emmett-Teller (BET) structural data of this adsorbent was determined by a Micromeritics ASAP 2020 V3.02 H analyzer. Its surface morphology was analyzed by scanning electron microscopy (SEM) (JSM-6460 LV) and a Fourier transform infrared (FTIR) analysis before and after the uptake of Zn^{2+} and Pb^{2+} was carried out using a SHIMADZU 8400S spectrometer.

Equilibrium modeling

This study was carried out by varying the metal ion solution concentration from 20 – 100 mg/L using a 50 mL volume. The adsorption of Pb^{2+} and Zn^{2+} were modeled using the Langmuir, Freundlich, Temkin and Dubinin-Radushkevich isotherms.

Langmuir

The Langmuir isotherm describes adsorbate-adsorbent system in which the extent of adsorbate coverage is limited to one monolayer of adsorbent (Langmuir, 1918) i.e. the definite sites on the surface can only hold one adsorbate molecules. It assumes that the energy associated with adsorption is the same at all the individual sites the adsorbates are assumed to be incapable of interacting with neighboring adsorbate molecules (Faust and Aly, 1983). The linear form of Langmuir model is given as Equation 3;

$$\frac{C_e}{q_e} = \frac{C_e}{q_o} + \frac{1}{q_o k} \ldots\ldots\ldots\ldots\ldots\ldots (3)$$

Where: $q_e$is the amount of metal ion adsorbed per unit mass of adsorbent (mg/g); q_o and k are the Langmuir constants relating to maximum adsorption capacity (mg/g) and energy of adsorption (L/mg), respectively while C_e is the equilibrium concentration (mg/L) of adsorbate in solution sample after adsorption.

Freundlich

The Freundlich isotherm does not consider all sites on the adsorbent surface to be equal i.e. adsorption surface with sites that have different energies of adsorption and are not equally available. The Freundlich isotherm unlike the Langmuir does not indicate an adsorption limit when coverage is sufficient to fill a monolayer (Freundlich, 1907). It assumes that, once the surface is covered, additional adsorbed species can still be accommodated. In other words, multilayer adsorption is predicted by this equation. The linear form is given by Equation 4;

$$\log q_e = \log k_f + \frac{1}{n}\log C_e \ldots\ldots\ldots\ldots\ldots (4)$$

Where: k_f and n are the Freundlich constants relating to adsorption capacity and adsorption intensity, respectively.

Temkin

The Temkin isotherm assumes that the heat of adsorption of all the molecules in layer decreases linearly with coverage due to adsorbent-adsorbate interactions, and that the adsorption is characterized by a uniform distribution of the bonding energies, up to some maximum binding energy. Its linear form is as represented by Equation 5;

$$q_e = B\ln K_T + B\ln C_e \ldots\ldots\ldots\ldots\ldots (5)$$

Where: $B = \frac{RT}{b}$ is the Temkin constant related to heat of sorption, b is the Temkin isotherm constant, K_T is the equilibrium binding energy constant, R is the universal gas constant and T is the absolute temperature (Gerente *et al.,* 2007).

Dubinin-Radushkevich (D-R)

The D–R model is a semi-empirical equation where adsorption follows a pore filling mechanism. It assumes that the adsorption has a multilayer characteristic (Hutson and Yang, 1997). The D-R isotherm model is usually applied to distinguish between the physical and chemical adsorption. Its linear form is expressed as Equation 6;

$$\ln q_e = \ln q_m - \beta\varepsilon^2 \ldots\ldots\ldots\ldots\ldots (6)$$

Where: q_e is the amount adsorbed, q_m is the D-R monolayer capacity, β is the constant related to sorption energy, ε = Polanyi potential related to equilibrium concentration (C_e) through Equation 7;

$$\varepsilon = RT\ln\left(1 + \frac{1}{C_e}\right) \ldots\ldots\ldots\ldots\ldots (7)$$

R = universal gas constant, T = Absolute temperature. A plot of $\ln q_e$ vsε^2, a straight line is obtained having a slope; β and an intercept $\ln q_m$. The value of β is related to the sorption energy, E through the relationship in Equation 8;

$$E = \frac{1}{\sqrt{(2\beta)}} \ldots\ldots\ldots\ldots\ldots (8)$$

Adsorption kinetics

The rates of the metal ions uptake are described by adsorption kinetics and this is an important characteristic which controls the residence time of adsorbate uptake at the solid-liquid interface (Xin-jiang *et al.,* 2014). The sorption kinetic study helps in the prediction of adsorption rates, which gives important information in the design of appropriate adsorption process. Quantifying the changes in adsorption with time therefore requires that an appropriate kinetic model is used (Santhi *et al.,* 2010). The kinetic models considered for the interpretation of the experimental data in this study are: pseudo-first order, pseudo-second order and Elovich. The linear forms of these equations are expressed in Equations 9, 10 and 11, respectively;

$$\log(q_e - q_t) = \log(q_e) - \frac{k_1}{2.303}t \ldots\ldots\ldots\ldots\ldots (9)$$

$$\frac{t}{q_t} = \frac{1}{k_2 {q_e}^2} + \frac{1}{q_e}t \ldots\ldots\ldots\ldots\ldots\ldots (10)$$

$$q_t = \left(\frac{1}{\beta}\right)\ln(\alpha\beta) + \left(\frac{1}{\beta}\right)\ln(t) \ldots\ldots\ldots\ldots\ldots (11)$$

where q_e and q_t are amounts of the adsorbates (mg/g) taken by the adsorbent at equilibrium and at time t, respectively, k_1 is a pseudo-firstorder sorption rate constant, k_2 is a pseudo-second order sorption rate

constant, α is the initial adsorption rate (mg/g/min) and β is the desorption constant (g/mg).

Adsorption mechanisms

The possibility of intra-particle diffusion is usually explored by using the intra-particle diffusion model represented by Equation 12;

$$q_t = K_{id}t^{1/2} + C \ldots\ldots\ldots\ldots\ldots (12)$$

Where: q_t is the quantity adsorbed at time t, K_{id} is the intra-particle diffusion rate constant and C is a constant that gives an idea about the thickness of the boundary layer.

The larger the value of C, the greater is the boundary layer effect. According to this model, a plot of q_t versus $t^{1/2}$ should be linear if intraparticle diffusion is involved in the adsorption process and if the plot passes through the origin then intraparticle diffusion is the sole rate-limiting step (Ozcan *et al.*, 2007). It has also been suggested that in instances when q_t versus $t^{1/2}$ is multilinear, two or more steps govern the adsorption process (Unuabonah *et al.*, 2007; Wu *et al.*, 2009).

Adsorption thermodynamics

For a better understanding of the effect of temperature on the adsorption of the metal ions, thermodynamic parameters such as change in Gibbs free energy ΔG, enthalpy change ΔH, and entropy change ΔS were studied. ΔH and ΔS were respectively evaluated from the slope and intercept of the plot of ln$K$ versus 1/T using Equation 13:

$$\ln K = \frac{\Delta S}{R} - \frac{\Delta H}{RT} \ldots\ldots\ldots\ldots\ldots (13)$$

While ΔG were calculated using Equation 14:

$$\Delta G = -RT \ln K \ldots\ldots\ldots\ldots\ldots (14)$$

R is the universal gas constant (8.314 J/mol/K), T is the absolute temperature (K) and K is the distribution coefficient which is a ratio of the concentration of the metal ion in the adsorbent and in the aqueous phase i.e. $K = \frac{C_{ads}}{C_{aq}}$.

Results and Discussion

XRD

XRD was done in the 2Θ range from 10° to 90°with a scanning step of 0.034°/71.6 s. The CS diffractogram (Fig. 1a) with major peak position at 29.6°, 48.8°, 47.8°, 39.6°, 43.3°, 36.2° was observed to match well with the data of calcite magnesian in the JCPDS file library 01-086-2335 but with a much similarity to the standard calcite (a polymorph of calcium carbonate) pattern as shown in Fig. 1b (RRUFF, 2014). This suggests the presence of Mg in trace amount.

XRF

It is evident from Tables 1 that calcium oxide is the major chemical constituent of CS, which is a peculiar component characteristic of calcareous shells. This finding is in concordance with the result of Awang-Hazmi *et al.* (2007) and Mustakimah *et al.* (2012) who analysed the chemical composition of cockle shell in Malaysia. Other constituents detected include; Aluminium oxide, Lutetium oxide, Yttrium oxide, etc.

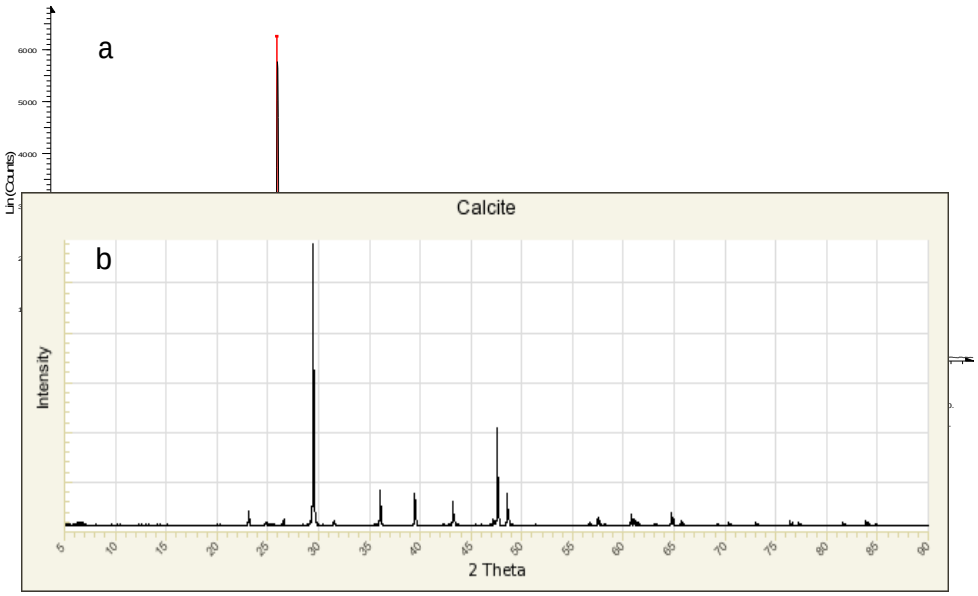

Fig. 1: XRD patterns of (a) Cockle Shell, and(b) Standard Calcite

Table 1: Chemical constituents of cockle shell

Compound	Al_2O_3	SO_3	CaO	Fe_2O_3	Y_2O_3	TiO_2	CeO_2	Sm_2O_3	Yb_2O_3	Lu_2O_3
Concentration (%)	1.7	0.14	97.44	0.096	0.40	0.037	0.073	0.05	0.04	0.089

Table 2: BET structural parameters of cockle shell

Surface Area (m^2/g)	Pore Volume (cm^3/g)	Pore Size (nm)
84.17	0.212	10.09

BET

The N_2 adsorption-desorption characterization was carried out and the structure data of CS are as given in Table 2. In the classification by the International Union of Pure and Applied Chemistry (IUPAC), pores are classified as micropores (< 2 nm diameter), mesopores (2 – 50 nm diameter) and macropores (>50 nm diameter). Based on this classification, it is seen that the CS powder ismesoporous with pore size of 10.09 nm.

SEM

The surface morphology of CS as revealed by SEM is presented in Fig. 2. Noticeable on the micrograph are some smooth jelly-like portions upon which irregularly-shaped particles are embedded and distributed which informs the coarse nature of this shell powder and its suitability for adsorption.

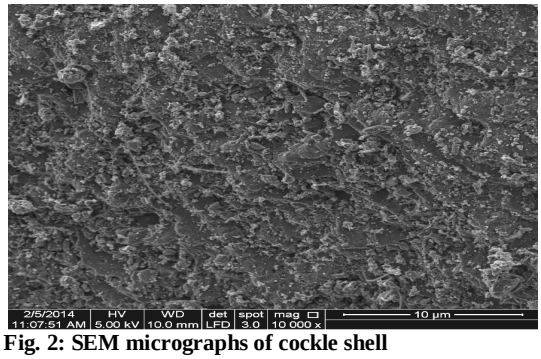

Fig. 2: SEM micrographs of cockle shell

FTIR

For the identification of the characteristic functional groups, which are instrumental in adsorption of the metal ions of interest, a Fourier Transform Infrared (FTIR) analysis was carried out. The strongest bands of the CS spectra before (Fig. 3a) and after adsorption (Figs. 3b&c) were observed in the range of 1500 – 600 cm^{-1}. The observed number of bands is an indication of the nature of the materials examined. In Fig. 4a, the broad peak at 3460.41 cm^{-1} results from O-H stretching vibration from the H_2O molecule, the highly intense peak at 1421.58 cm^{-1} is characteristic of C-O asymmetric stretching vibration, while the bands centered around 875.1 cm^{-1} and 711.76 cm^{-1} are assigned to the out-of-plane bending vibration and in-plane bending vibration of the CO_3^{2-}, respectively. After Pb^{2+} loading onto CS (Fig. 3b), an increase in intensity of the bands was observed with peak shifts (1421.58 to 1423.51 cm^{-1} and 3460.41 to 3466.2 cm^{-1}), while after Zn^{2+} uptake (Fig. 3c), a reduction in the intensity of all the bands, band shifts from 2511.4 cm^{-1} and 3460.41 cm^{-1} to 2513.33 cm^{-1} and 3466.2 cm^{-1} respectively and a split of the peak at 1421.58 cm^{-1} into peaks at 1423.51 cm^{-1} and 1471.74 cm^{-1} were observed. Also noticeable is the appearance of a band at 1084.03 cm^{-1} which is characteristic of symmetric stretching vibration of CO_3^{2-}. These changes are possibly due to some ion exchange behavior of the CS due to its interactions with the metal ions.

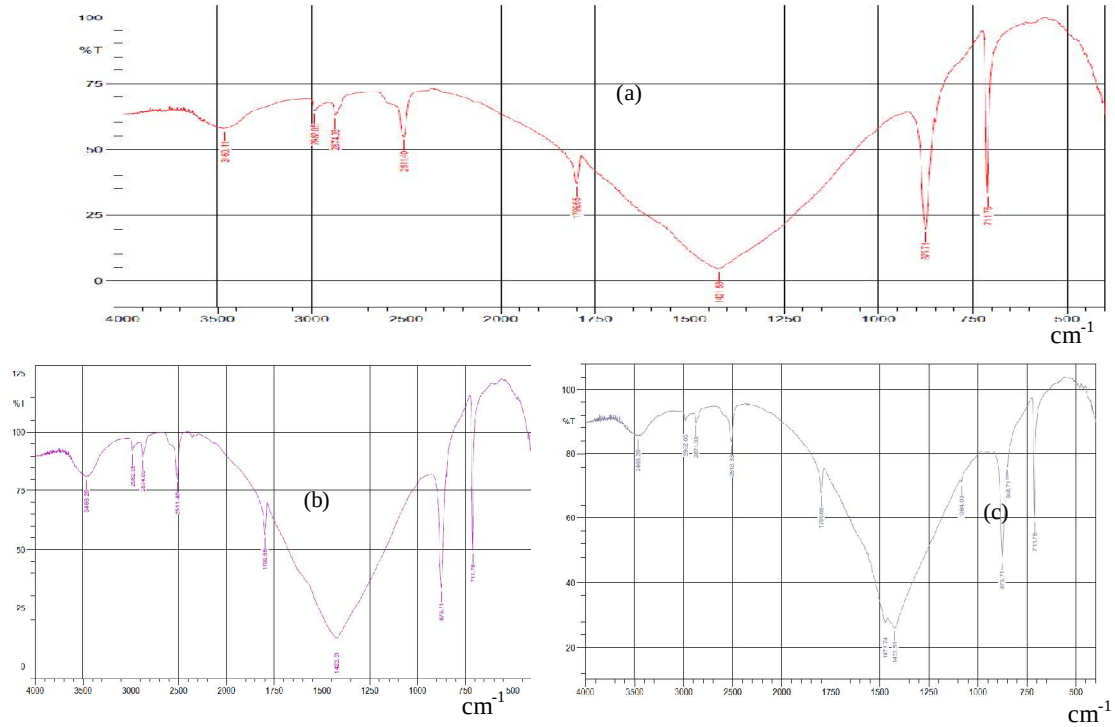

Fig. 3: FTIR spectra of cockle shell (a) before adsorption (b) after Pb^{2+} uptake (c) after Zn^{2+} uptake

Effect of initial metal ion concentration

Initial adsorbate concentration is generally known to provide the necessary driving force to overcome the resistance to the mass transfer of adsorbate between the aqueous phase and the solid phase (Yeddou and Bensmaili, 2007). The influence of initial concentrations of Pb^{2+} and Zn^{2+} sorption by CS powders investigated revealed that as the initial concentration was increased, the amount of these metal ions adsorbed per gram of the CS powder also increased (Fig. 4). The uptake of Pb^{2+} ion increased from 2.53 mg/g to 24.66 mg/g while that of Zn^{2+} ion increased from 2.24 mg/g to 21.70 mg/g. This phenomenon can be explained thus; at low concentrations, there was only a little driving force which transferred the metal ions onto the readily available sites of the adsorbents. As the concentration was increased, the driving force also increased which then enhanced the interaction between the adsorbates and adsorbents thereby causing an increase in the quantity adsorbed. A similar trend was observed on some heavy metals sorption using calcareous shells of animal origin (Edu *et al.,* 2012) and flame of the forest pods (Aiyesanmi *et al.,* 2013).

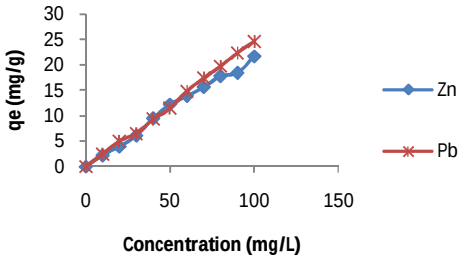

(vol. = 50 mL, pH = 4, dose = 0.2 g,time = 180 min, T = 32 ± 1 ^{0}C and 200 rpm)

Fig. 4: Effect of initial metalion concentration

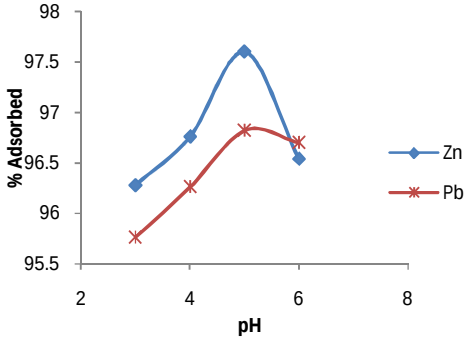

(vol. = 50 mL, Co = 50mg/L, dose = 0.2 g,time = 180 min, T = 32 ± 1 ^{0}C and 200 rpm)

Fig. 5:Effect of solution pH

Effect of pH

Calcareous shells are known to contain $CaCO_3$ as their major component and this is capable of imparting alkalinity to whichever system in which they are being used. Thus, any aqueous solution equilibrated with calcareous shells become more basic. This can be represented by equations 15 and 16 (Brown *et al.,* 1991);

$$CaCO_3 \rightarrow Ca^{2+} + CO_3^{2-} \quad \ldots\ldots\ldots\ldots (15)$$

$$CO_3^{2-} + H_2O \rightarrow HCO_3^{-} + OH^{-} \quad \ldots\ldots\ldots\ldots (16)$$

The hydrolysis of $CaCO_3$ produces basic solution due to Ca^{2+} and OH^-ions, responsible for increase in pH of the solution and this in turn affects the surface charges of the adsorbents. This alkalinity was confirmed, as the measured pH of the CS powder gave 9.576. Adjusting the solution pH is therefore paramount in obtaining greater removal efficiency for metal ions. Presented in Fig. 6 is the result obtained by varying the solution pH. An increase in the pH of the metal ion solutions brought about an increase in the percentage adsorbed. Maximum percentage adsorption of about 96.82% was observed for the Pb^{2+} metal ion at pH 5, which decreased slightly to 96.70% with a further increase of the pH to 6, while about 97.60% of the Zn^{2+} metal ion was maximally adsorbed at pH 5, which reduced to 96.54% at a pH of 6. These results are in conformity with the results of Abdus-Salam and Adekola (2005) and Genson *et al.* (2012)where Pb^{2+} adsorption was practically total (100%) at pH 5 for the whole range of concentration studied and Kathrine and Hans(2007) who reported Zn^{2+} to be sensitive to maximum sorption onto coir at pH 4.5.

The trend observed with the pH variation as seen in Fig. 5 can be explained thus; at low pH values, hydrogen ion (H^+) abound much in the solutions increasing the competition for the available binding sites on the CS powder with the metal ions, which then restricted the approach of the metal cations of interest through repulsive forces, consequently limiting the percentage removal of these metal ions (Low *et al.,* 1993). An increase in the pH of the solutions brought about a corresponding increase in deprotonation, thereby making it easier for the cations to approach the binding sites on the shell powder. A further increase beyond pH 5 led to precipitation of the hydroxide form of the metals ions; therefore true adsorption was not feasible; thus there was a decline in the percentage of metal ions adsorbed (Genson*et al.,* 2012).

Effect of contact time

The graphical representation of the results obtained due to the varied time of contact of the metal ions and shell powder (Fig. 6) revealed the rapid increase in the percentage of both metal ions adsorbed at the early stage of the experiment. Just in about 5 minutes into the experiment, 59.74% of Zn^{2+} ion and 51.54% of Pb^{2+} were already adsorbed. This increase continued until equilibrium was attained in 90 minutes with percentage sorption of about 96.2% and 98.0% for Zn^{2+} and Pb^{2+} respectively, after which an intermittent decrease and increase was observed due to desorption and adsorption.

The rapid removal of the metal ions observed at the early stage of the experiment could be attributed to the instantaneous utilization of the readily available adsorption sites on the adsorbent's surface. As time went

by, the adsorption sites gradually became saturated, diminishing the concentration of the metal ion in the solution and the sorption experiment tended to be more unfavourable.

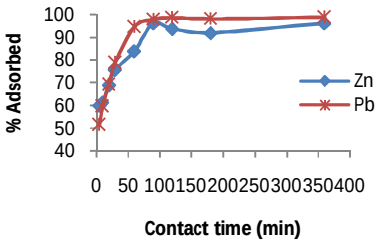

(vol. = 50 mL, Co = 50mg/L, dose = 0.2 g, pH = 5, T = 32 ± 1 ^{0}C and 200 rpm)

Fig. 6: Effect of contact time

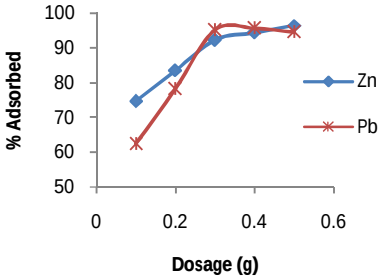

(vol. = 50 mL, Co = 50mg/L, time = 90 minutes, pH = 5, T = 32 ± 1 ^{0}C and 200 rpm)

Fig. 7: Effect of dosage

Effect of dosage

The amount of available surface area under an effectively constant metal surface is one of the most significant experimental variables affecting contaminant reduction rate. The effect of varying the adsorbent dosage on the metal ions sorption is shown in Fig. 7.With dosage increase from 0.1 g to 0.3 g, Zn^{2+} removal increased from 74.72% to 92.44% while Pb^{2+} removal increased from 62.5% to 94.62%. Further increase in the dosage resulted to an insignificant increase in the metal ion adsorbed. This could be due to the higher number of free sites and lesser number of metal ions.

Effect of temperature

The influence of variation of temperature on the adsorption of Pb^{2+} and Zn^{2+} ions by CS examined under temperature range of 30 to 60 °C revealed that the adsorption increased with increase in temperature (Fig. 8). This is because at higher temperature, the diffusion of metal ions through the shell pores is faster and can proceed to a larger extent (Qadeer and Hanif, 1994; Bharathi and Ramesh, 2012). The increase in adsorption upon increasing the temperature indicates an endothermic nature for each of the adsorption processes.

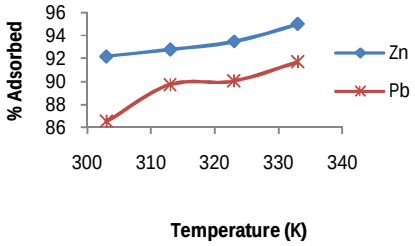

(vol. = 50 mL, Co = 50mg/L, time = 90 minutes, pH = 5, dose = 0.3 g and 200 rpm)

Fig. 8: Effect of temperature

Adsorption isotherm

The adsorption isotherm data were generated from an experiment carried out by varying the metal ion solution concentration from 20 to 100 mg/L using a 50 mL volume and maintaining the optimum values obtained from the process conditions. The results obtained are presented in Fig. 9 (a – d).The isotherm parameters derived from Fig. 9 (a – d) are summarized in Table 3.The data show that the sorption of Zn^{2+} ion was best correlated (R^2> 0.98) with the Freundlich model as compared with Langmuir, Temkin and D-R equations while the sorption of Pb^{2+} ion was best described by the D-R isotherm due to its highest correlation coefficient value (R^2 = 0.979). The value of n > 1 as estimated from the Freundlich model is an indication of a high affinity between the Zn^{2+} and the CS revealing that the adsorption is a favourable process (Stevensand Nnabuk, 2009). The estimated D-R energy of sorption (E = 0.845kJ/mol) suggests that the Pb^{2+} sorption process is governed by physical adsorption mechanism (E < 8kJ/mol) (Monika *et al*., 2009).

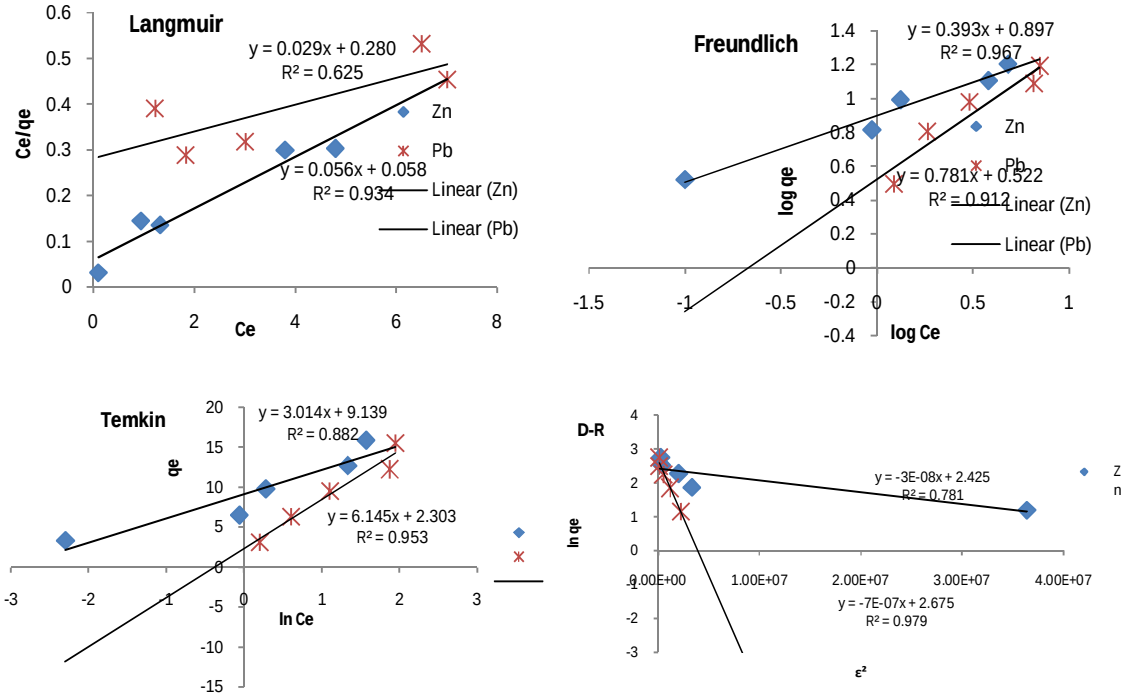

Fig. 9 (a – d): Langmuir, Freundlich, Temkin and D-R isotherm plots for Pb^{2+} and Zn^{2+} uptake

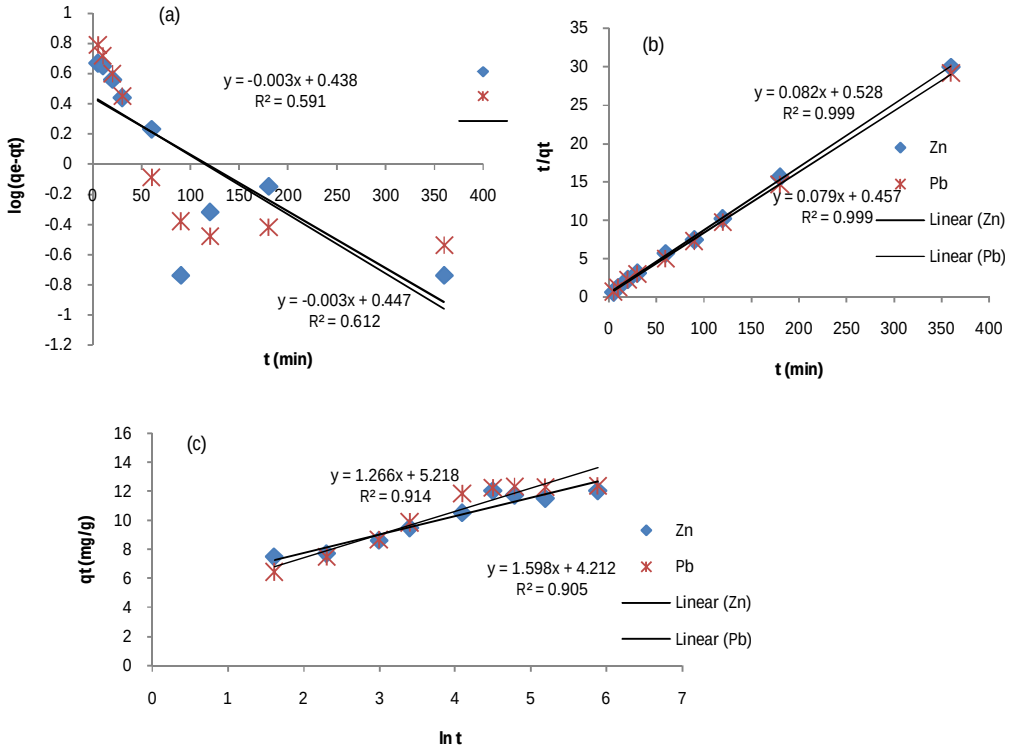

Fig. 10: Pseudo-first order (a), Pseudo-second order (b) and Elovich (c) Kinetic plots

Adsorption kinetics

The kinetics of the adsorption process was evaluated by pseudo-first order, pseudo-second order and Elovich models while the adsorption mechanism was evaluated by the intra-particle diffusion model. The linear plots obtained from these models are presented in Fig. 10, while the rate constants, expected metal uptake and correlation coefficients are presented in Table 4. The pseudo-first order theoretical q_e values (4.09 mg/g for Zn^{2+} and 2.74 mg/g for Pb^{2+}) evaluated from Fig. 10a when compared with the experimental q_e values (12.02 mg/g for Zn^{2+} and 12.24 mg/g for Pb^{2+}) differ widely. Also the correlation coefficient values (R^2) values were low, which showed that pseudo first order equation of Lagergren does not fit well with whole range of contact time.The pseudo-second order model on the contrary showed a high linearity as observed in Fig. 10b and the consistency in the evaluated q_e values and the experimental q_e (Table 4) is an indication that the experimental data fitted well into the pseudo-second order model. The product $k_2 q_e^2$ is the initial sorption rate, h. Pb^{2+} ion exhibited a more continuous and higher initial sorption rate of 2.188 mg/g/min over the Zn^{2+} ion.

A straight line plot of q_t versus $ln\ t$ indicates the applicability of Elovich model but that is not the case here as seen from Fig. 10c. The correlation coefficients and the kinetic data calculated from the intercepts and slopes of the plots are also shown in Table 4.Considering the closeness of the experimentally observed and evaluated equilibrium adsorption capacity for the pseudo-second order model (Table 4), in addition to its large correlation coefficients, it can be said that both Zn^{2+} and Pb^{2+} adsorptions were not adequately described by pseudo first order, Elovich and intra-particle diffusion models. Thus the adsorption system can be said to follow the pseudo-second order model.

Table 4:Pseudo-first order, pseudo-second order and Elovich kinetic data

Model	Parameters	Values	
		Zn^{2+}	Pb^{2+}
Pseudo-First order	$q_e\ (mg/g)$	4.09	2.74
	$k_1\ (min^{-1})$	6.91×10^{-3}	6.91×10^{-3}
	R^2	0.612	0.591
Pseudo-Second order	Evaluated $q_e\ (mg/g)$	12.20	12.66
	Experimental $q_e\ (mg/g)$	12.02	12.24
	$k_2\ (g/mg/min)$	1.27×10^{-2}	1.37×10^{-2}
	$h\ (mg/g/min)$	1.894	2.188
	R^2	0.999	0.999
Elovich	$\alpha\ (mg/g/min)$	78.014	22.309
	$\beta\ (g/mg)$	0.789	0.625
	R^2	0.914	0.905

Table 5:Intra-particle diffusion model data

Stage	Zn^{2+}			Pb^{2+}		
	K_{id}(mg/g/min$^{1/2}$)	C	R^2	K_{id}(mg/g/min$^{1/2}$)	C	R^2
1	0.624	5.896	0.964	1.034	4.136	0.997
2	0.082	10.54	0.330	0.034	11.80	0.481

Table 6: Thermodynamic parameters for Zn^{2+} adsorption by cockle shell (CS-Zn^{2+})

Adsorbate	$\Delta G\ (kJ/mol)$				ΔH(kJ/mol)	ΔS(kJ/mol/K)
	30°C	40°C	50°C	60°C		
Zn	- 6.219	- 6.651	- 7.156	- 8.151	12.75	62.27
Pb	- 4.683	- 5.642	- 5.913	- 6.650	13.83	61.49

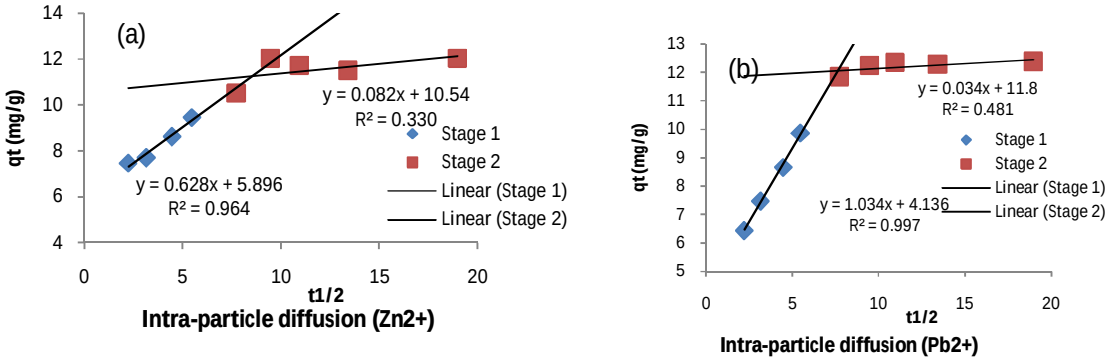

Fig. 11: Intra-particle diffusion plots (a, b)

Adsorption mechanism

In order to determine whether the overall rate of adsorption was controlled by intra-particle diffusion i.e. the movement of the adsorbate molecules into the interior of the adsorbent particles, the Weber-Morris intra-particle diffusion model was used. The intra-particle diffusion plots are presented in Fig. 11. The intra particle diffusion rate constants (K_{id}) calculated from the slope and the value of intercept(C) are presented in Table 5. The larger intercept values suggest that intra-particle diffusion has a lesser role to play compared with surface diffusion. The multi-linearity observed is an indication that two steps occurred in the adsorption process. The sharply rising part is the external surface diffusion stage while the second part is the gradual diffusion stage where intra-particle diffusion occurs. The deviation of the lines from the origin and the low R^2 values of the gradual diffusion stage suggest that intra-particle diffusion is not the sole rate limiting step.

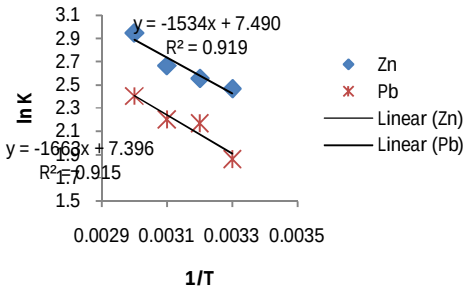

Fig. 12: Van't Hoff Plots

Adsorption thermodynamics

The thermodynamic parameters evaluated from the Van't Hoff Plot (Fig. 12)are presented in Tables 6.The negative values of ΔG observed at all the temperature considered indicates the feasibility and spontaneity of the adsorption processes. The ΔG values increased with an increase in temperature which reflects a more favourable adsorption at high temperatures. The positive ΔH values suggest that the adsorptions of the metal ions are endothermic in nature while the positive values of ΔS suggest a high degree of disorder and randomness at the adsorbent-adsorbate interface during the fixation of the adsorbate ions (Zn^{2+} and Pb^{2+}) on the adsorbent.

Conclusion

It was clearly established from the study that cockle shell is a good adsorbent for the removal of Pb^{2+} and Zn^{2+}ions in aqueous mediawithout special pretreatment.The removals of the metal ions were clearly influenced by the operational parameters vis-à-vis concentration, pH, contact time, dosage and temperature. Freundlich isotherm adequately described the sorption of Zn^{2+}, while the sorption of Pb^{2+} was adequately interpreted by D-R isotherm. The thermodynamics and kinetics studies revealed the endothermic nature of the processes which followed pseudo-second order kinetics.

Acknowledgements

The effort of Dr. Bello Olugbenga of the Department of Pure and Applied Chemistry, Ladoke Akintola University of Technology through whom the BET analysis was carried is greatly appreciated.

References

Abdus-salam N&Adekola FA 2005.The influence of pH and adsorbent concentration on adsorption of lead and zinc on a natural goethite.*African Journal of Science and Technology (AJST) Science and EngineeringSeries*, 6(2): 55 – 66.

Aiyesanmi AF, Okoronkwo AE &Akinmolayan, BM 2013.Equilibrium Sorption of Lead and Nickel from Solutions by Flame of the Forest (*Delonixregia*) Pods: Kinetics and Isothermic Study. *Journal of Environmental Protection*, 4: 261-269.

Asi H &Gautam A 2013.Cadmium biosorption potential of shell dust of the fresh water invasive snail (*Physaacuta*).*Journal of Environmental Chemical Engineering*,1: 574–580.

Awang-Hazmi AJ, Zuki ABZ, Nordin MM,Jalila A &Norimah Y 2007. Mineral composition of the cockle (*Anadaragranosa*) shells of west coast of peninsular Malaysia and its potential as biomaterial for use in bone repair. *Journal of Animal and Veterinary Advances*,6(5): 591-594.

Badmus MAO, Audu TOK &Anyata BU 2007.Removal of Lead ion from Industrial Wastewaters by Activated Carbon Prepared from Periwinkle Shells (*Typanotonusfuscatus*).*Turkish Journal of Engineering and Environmental Science*, 31: 251 – 263.

Bharathi KS & Ramesh SP 2012. Equilibrium, thermodynamic and kinetic studies on adsorption of a basic dye by *Citrulluslanatus*rind. *Iranica J. Energy and Environ.*, 3(1): 23-34.

Brown TL, LeMay HE &Bursten BE 1991. Chemistry: *The Central Science*, 5th ed., New Jersey: Prentice Hall, 495.

Dahiya S, Tripathi RM &Hedge AG 2008.Biosorption of lead and copper from aqueous solutions by pre-treated crab and arca shell biomass.*Bioresource Tech.*, 99: 179–187.

Edu I, Ubong E, Eduok U& Joseph E 2012.Heavy metals sorption potential of calcareous shells of animal origin.*Int. J. Chemical, Environmental and Pharmaceutical Res.*,3(3): 184-194.

Faust DS & Aly MO 1983.*Chemistry of Wastewater Treatment*.Butterworthworts. Boston.

Freundlich H 1907. Ueber die Adsorption in Loesungen Z. *Physik Chemistry*,57: 385 – 470.

Genson M, CharlesOO & Gerald KM 2012.Kinetic and equilibrium study for the sorption of pb(ii) ions from aqueous phase by water hyacinth (*Eichhorniacrassipes*). *Bull. Chem. Soc. Ethiopia*, 26(2): 181-193.

Gerente C, Lee, VKC, Le Cloirec P & McKay G 2007. Application of chitosan for the removal of metals from wastewaters by adsorption – mechanisms and models review.*Critical Reviews in Envtal. Sci.& Tech.*, 37: 41–127.

Gifford S, Dunstan RH, O'Connor W, Koller CE & MacFarlane GR 2006. Aquatic Zoo-remediation: Deploying animals to remediate contaminated aquatic environment. *Trends in Biotech*, 25: 60–65.

Hutson ND & Yang RT 1997.Theoretical basis for the Dubinin–Radushkevitch (D–R) adsorption isotherm equation. *Adsorption,* 3: 189–195.

Kathrine C & Hans C 2007.Sorption of zinc and lead on coir.*Bioresource Tech.,* 98: 89–97.

Langmuir I 1918.The adsorption of gases on plane surfaces of glass, mica and platinum.*J. American Chem. Soc.,* 40(9):1361 – 1403.

Liu Y, Sun C, Xu J & Li Y 2009. The use of raw and acid pretreated *Bivalve mollusc* to remove metals from aqueous solutions. *Journal of Hazardous Material,* 168: 156–162.

Low KS, Lee CK & Lee KP 1993.Sorption of copper by dye-treated oil palm fibre.*Bioresource Tech.,* 44: 109-112.

Monika J, Garg V&Kadirvelu K 2009.Chromium (VI) Removal from aqueous solution, using sunflower stem waste.*Journal of Hazardous Materials,* 162: 365 – 372.

Mustakimah M, Suzana Y &Saikat M 2012.Decomposition study of calcium carbonate in cockle shell.*J. Engineering, Sci. and Tech.,* 7(1): 1 – 10.

Ozcan A, Ozcan AS &Gok O 2007.Adsorption kinetics and isotherms of anionic dye of reactive blue 19 from aqueous solutions onto DTMA-sepiolite. In: A.A. Lewinsky (ed.), hazardous materials and wastewater–treatment, removal and analysis.*Nova Science Publishers*, New York.

Pena-Rodriguez S, Fernandez-Calvino D, Novoa-Munoz JC, Nunez-Delgado A, Fernandez-Sanjurjo MJ & Alvarez-Rodriguez A 2010. Kinetics of Hg(II) adsorption and desorption in calcined mussel shells. *J. Hazardous Material,* 180: 622–627.

Qadeer R &Hanif J 1994.Kinetics of zirconium ions adsorption on activated charcoal from aqueous solution. *American J. of Biochem. and Biotech.* 3(2): 34-43.

RRUFF 2014. Calcite [Online]. Available from: http://rruff.info/Calcite/R040078. Accessed: 13-06-2014.

Santhi T, Manonmani S &Smitha T 2010.Kinetics and Isotherm Studies on Cationic Dyes Adsorption onto *AnnonaSqumosa*seed activated carbon.*Int. J. of Engineering Sci. and Tech.,* 2(3): 287-295.

Stevens AO &Nnabuk OE 2009.Studies on the use of oyster, snail and periwinkle shells as adsorbents for the removal of Pb^{2+} from aqueous solution.*E-Journal of Chemistry,*6(1):213-222.

Unuabonah EI, Adebowale KO &Olu-Owolabi BI 2007.Kinetic and thermodynamic studies of the adsorption of lead (II) ions onto phosphate-modified kaolinite clay.*J. Hazardous Material,* 144: 386–395.

Wikipedia 2013.Heavy Metals.[Online]. Available from:http://en.wikipedia.org/wiki/Heavy_metal_chemistry. Accessed: 16-12-2013.

Wu FC, Tseng RL &Juang RS 2009.Initial behavior of intraparticle diffusion model used in the description of adsorption kinetics.*Chem. Engineering J.,* 153: 1–8.

Xin-jiang H, Yun-guo L, Guang-ming Z, Hui W, Xi H, An-wei C, Ya-qin W, Yi-ming G, Ting-ting L, Lu Z, Shao-heng L & Xiao-xia Z 2014.Effect of aniline on cadmium adsorption by sulfanilic acid-grafted magnetic graphene oxide sheets.*J. Colloid and Interface Sci.,*426: 213–220.

Yeddou N &Bensmaili A 2007.Equilibrium and kinetic modeling of iron adsorption by eggshells in a batch system: Effect of temperature. *Desalination,* 206(1–3): 127–134.